Metal-Ion-Mediated Allosteric Triggering of Yeast Pyruvate Kinase. 1. A Multidimensional Kinetic Linked-Function Analysis†

Andrew D. Mesecar‡,§ and Thomas Nowak*

Department of Chemistry and Biochemistry, University of Notre Dame, Notre Dame, Indiana 46556

Received November 20, 1996; Revised Manuscript Received March 5, 1997⊗

ABSTRACT: Regulation of the glycolytic pathway is considered to be primarily achieved by the carbon metabolites resulting from glucose metabolism [e.g., fructose 1,6-diphosphate (FDP), phosphoenolpyruvate (PEP), and citrate] and by the ATP charge of the cell. The divalent cations (e.g., Mg^{2+} and Mn^{2+}) have not been considered as having regulatory roles in glycolysis, although they are involved in almost every enzyme-catalyzed reaction in the pathway. Using a kinetic linked-function analysis of steady-state kinetic data for the interactions of PEP, FDP, and Mn^{2+} with yeast pyruvate kinase (YPK), we have found that the divalent metal is the principal trigger of the allosteric responses observed with this enzyme. The interaction of Mn^{2+} to YPK enhances the interaction of FDP by −1.6 kcal/mol and the interaction of PEP by −2.8 kcal/mol. The simultaneous interaction of all three of these ligands to YPK is favored by −4.3 kcal/mol over the sum of their independent binding free energies. Surprisingly, the binding of the allosteric activator FDP does not directly influence the binding of the substrate PEP since a coupling free energy near zero was calculated for these two ligands. Thus, communication between the PEP and FDP sites occurs structurally through the metal by an allosteric relay mechanism. These conclusions are supported by results of a thermodynamic linked-function analysis of direct binding data for the interactions of PEP, FDP, and Mn^{2+} with YPK [Mesecar, A. D., & Nowak, T. (1997) *Biochemistry* (following paper in this series)]. Our findings raise important questions as to the possible roles of divalent metals in modulating multiligand interactions with YPK and in the regulation of the glycolytic pathway.

Glycolysis is an essential metabolic pathway in virtually all organisms. The component reactions of this pathway are practically invariant in nature, and the enzymes that catalyze these reactions show a high degree of evolutionary conservation (Fothergill-Gillmore, 1986; Farber & Petsko, 1990). Since the glycolytic pathway is a crucial component of energy metabolism in cells, an understanding of its regulatory elements is of major interest.

One site of regulation of the glycolytic pathway is by the enzyme pyruvate kinase (PK).[1] This enzyme catalyzes the last energy-producing step of glycolysis where ATP and pyruvate are formed from the transfer of a phosphoryl group from phosphoenolpyruvate (PEP) to adenosine 5′-diphosphate (ADP):

$$H^+ + PEP + M(II)ADP \xrightleftharpoons{M(I),\ M(II)} Pyruvate + M(II)ATP$$

The reaction is essentially irreversible, in favor of ATP and pyruvate formation, and has an absolute requirement for both a monovalent cation, usually K^+, and divalent cations, typically Mg^{2+} or Mn^{2+}. Regulation of PK activity is a necessity for preventing substrate cycling between PEP and pyruvate during gluconeogenesis.

Regulation of PK activity is accomplished by a variety of mechanisms. In mammals, four isozymes of PK that have different kinetic properties exist. These isozymes, designated M1, M2, R, and L, are expressed in different tissues. Type M1 is nonallosterically regulated and exists in skeletal muscles, heart, and brain, where glycolysis is the principal metabolic pathway. Type L pyruvate kinase is found in liver where metabolic alternation between glycolysis and gluconeogenesis frequently occurs. Type L PK shows sigmoidal kinetics for PEP and is allosterically regulated by the heterotropic activator fructose 1,6-diphosphate (FDP). The other isozymes (M2 in kidney, lung, adipose and early fetal tissues, and R in erythrocytes) are also allosterically regulated by FDP and PEP.

Studies concerning the regulation of pyruvate kinase activity have focused primarily on the interactions of PEP and FDP with the enzyme. However, pyruvate kinase activity from a number of sources has also been shown to be allosterically activated by protons and the required monovalent and divalent cations (Rhodes et al.,1986; Kinderlerer et al., 1986; Rozengurt et al., 1969; Waygood & Sanwal, 1974). These studies and others have shown that the allosteric kinetic responses of pyruvate kinase involve the interactions of many ligands and that PEP and FDP are not the only ligands influencing the kinetic responses of PK.

Mg^{2+} is generally considered to be the physiological activator of PK. The nonallosteric muscle enzyme requires two divalent cations per subunit for catalysis (Baek & Nowak, 1982), and Mn^{2+} and Co^{2+} can substitute for Mg^{2+} (Nowak & Suelter, 1981). Pyruvate kinase isolated from

† Supported by a grant from the National Institutes of Health (DK 17049).

* Author to whom correspondence should be addressed.

‡ Present address: Department of Molecular and Cell Biology, University of California at Berkeley, Berkeley, CA 94596.

§ Recipient of a GAANNP fellowship from the United States Department of Education.

⊗ Abstract published in *Advance ACS Abstracts,* May 15, 1997.

[1] Abbreviations: PK, pyruvate kinase; YPK, yeast pyruvate kinase; ADP, adenosine 5′-diphosphate; PEP, phospho(enol)pyruvate; FDP, fructose 1,6-diphosphate; MES, 2-(*N*-morpholino)ethanesulfonic acid.

S0006-2960(96)02869-3 CCC: $14.00

Mytilus edulis l (Zwaan et al., 1975), *Mucor rouxii* (Passeron & Terenzi, 1970), *Concholepas concholepas* (Gonzalez et al., 1984), and *Thiobacillus versutus* A2 (Klein & Charles, 1989) show sigmoidal responses in activity with respect to Mg^{2+} and PEP concentrations. In the presence of Mn^{2+}, however, the interaction of PEP with PK is hyperbolic. These results suggest that the interaction of Mn^{2+} is different than the interaction of Mg^{2+} with the enzyme from these organisms and that Mn^{2+} may "mimick" the allosteric effect of FDP, AMP, or G6P. In a kinetic study with PK isolated from *Concholepas concholepas*, it is proposed that the Mn^{2+} activated enzyme follows an ordered sequential kinetic mechanism and that the Mg^{2+} activated enzyme in the presence of FDP follows a random kinetic mechanism (Carvajal, 1985).

The differences in the nature of Mg^{2+} and Mn^{2+} activated reactions of pyruvate kinase from a variety of sources suggest a possible regulatory role for the divalent metal. Since the role of the enzyme-bound divalent metal in the allosteric activation of regulated pyruvate kinase is currently unknown, it was of interest to examine the effects of the divalent metal on the allosteric kinetic responses of PK isolated from *Saccharomyces cerevisiae*. Yeast pyruvate kinase (YPK) is a tetramer with four identical subunits (Burke et al., 1983). The Mg^{2+} activated enzyme exhibits a sigmoidal dependence of velocity on PEP concentration that becomes hyperbolic in the presence of the activator FDP. YPK has also been shown to be allosterically activated by K^+, NH_4^+, and Mg^{2+} (Hunsley & Suelter, 1969). Differences in the Mg^{2+}, Mn^{2+}, and Co^{2+} activated enzyme have been described by Ford and Robinson (1976). The differences among various divalent activators are quantitative with variations in V_{max} and K_M values, although the qualitative effects on activation appear similar. The following study was undertaken in order to more fully describe the nature of the regulatory responses of yeast pyruvate kinase to PEP, FDP, and free Mn^{2+} concentrations and to quantitate the magnitude of these interactions.

A linked-function analysis is an ideal approach for investigating the relationships between FDP, PEP, and free Mn^{2+} activation of YPK. The approach utilizes the concept of "free energy" in quantitation of the magnitude of the interactions between multiple ligands bound to a single protein (Reinhart, 1983, 1985, 1988). By considering protein−ligand interactions from a free-energy standpoint, insight into the molecular forces that modulate these interactions may be obtained (Weber, 1972, 1975). Without consideration of the energetics involved in multiple ligand binding, knowledge of the structural origins of these interactions may not be given to proper physical interpretation. At present, three high resolution crystal structures exist for pyruvate kinase (Larsen et al., 1994; Allen & Muirhead, 1996; Mattevi et al., 1996). Only the rabbit muscle M1 isozyme has been solved in the presence of ligands, and this enzyme is nonallosterically regulated (Larsen et al., 1994). We have focused our attention on the energetics of ligand interactions to the allosterically regulated yeast enzyme in anticipation of an eventual crystal structure.[2]

[2] The crystal structure of yeast pyruvate kinase has recently been elucidated in collaboration with Dr. Barry Stoddard, Fred Hutchinson Cancer Research Center.

EXPERIMENTAL PROCEDURES

Materials. Pyruvate kinase was overexpressed and purified as described in the following paper (Mesecar & Nowak, 1997a). KCl, $MgCl_2$, $MnCl_2$, dicyclohexylammonium ADP, monocyclohexylammonium PEP, tetracyclohexylammonium FDP, disodium NADH, glycerol, and MES were purchased from Sigma. Lactate dehydrogenase from rabbit muscle was obtained from Boehringer-Mannheim. All reagents were of the highest purity available, and distilled, deionized water was used throughout.

Pyruvate Kinase Assay. Yeast pyruvate kinase activity was measured by a continuous assay coupled to lactate dehydrogenase (LDH). The change in absorbance at 340 nm due to oxidation of NADH was measured using either a Gilford Model 240, 250, or 260 thermostated spectrophotometer. Specific activity assays contained in 1.00 mL: MES (100 mM), glycerol (5%), KCl (200 mM), $MgCl_2$, (15 mM), ADP (5 mM), PEP (5 mM), FDP (1 mM), NADH (175 μM), LDH (20 μg), and YPK (0.5−0.7 μg). A baseline was established for each reaction after the addition of LDH. Reactions were started by the addition of 10 μL of YPK and were performed at 24 ± 1 °C. The specific activity of YPK is expressed as micromoles of NADH oxidized per milliliter per minute per milligram of pyruvate kinase (units per milligram). The concentration of purified YPK was determined by its absorbance at 280 nm using an extinction coefficient, ϵ_{280}, of 0.51 $(mg/mL)^{-1}$ (Yun et al., 1976).

Kinetic studies were performed as described for the specific activity determinations except for the following: manganese was substituted for magnesium and its concentrations were varied and PEP and FDP concentrations were also varied at fixed variable concentrations of substrates or activators as described in the text. Unless noted, the total ADP concentration was maintained at 5 mM. Free manganese concentrations were calculated from the following equation: $K_D = ([ADP]_{free}[Mn^{2+}])/[Mn{-}ADP]_{bound}$ where K_D is the dissociation constant for the manganese−ADP complex. The K_D was determined in our laboratory to be 0.125 mM under conditions of this assay.

Fluorescence Measurements. The steady-state intrinsic fluorescence intensity of YPK was measured on a SLM 8100 fluorimeter thermostated at 24 ± 1 °C. The excitation wavelength was 295 nm, with a band width of 1 nm and the emission wavelength was 334 nm with a band width of 2 nm. Fluorescence titrations were performed by sequentially adding 1−10 μL aliquots of a concentrated stock solution of PEP to either 900 μL of the YPK complex, which contained MES (100 mM), glycerol (5%), KCl (200 mM), and YPK (0.068 mg/mL), or to the YPK−ADP complex, which contained the same mixture as the YPK complex plus 9.1 mM ADP. Neither complex contained Mn^{2+}. The percent fluorescence quenching, Q, was calculated from the following formula: $Q = [(F - F_o)/F_o]100$, where F is the fluorescence intensity of YPK in the presence of a titrating ligand and F_o is the fluorescence intensity of YPK in the absence of the ligand. F was corrected for fluorescence intensity changes due to dilution. Dissociation constants for PEP were obtained by fitting the calculated values of Q to the following formula: $Q = Q_M/(1 + K_D/[PEP])$, where Q_M is the percent maximal quenching and K_D is the dissociation constant for PEP.

Data Analysis. Steady-state kinetic rates were determined by measuring the slope of the tangent to the reaction progress curve. Progress curves were linear at least over the first several minutes, unless otherwise indicated. In those cases, a small transient lag prior to the steady-state velocity is observed. The initial velocity data were fit to both the Michaelis−Menten equation

$$v/V_{max} = 1/(1 + K_M/[S]) \quad (1)$$

and to the Hill equation

$$v/V_{max} = 1/(1 + (K_M/[S])^{n_H}) \quad (2)$$

for the determination of the apparent Michaelis constants (K_M), Hill coefficients (n_H), and maximal velocity (V_{max}) for PEP, FDP, and Mn^{2+}, respectively. The dependence of the apparent K_M of each ligand on the concentrations of one or both of the other ligands was evaluated by fitting data to the following equations as described in the text:[3]

$$K_A = K_A^{\circ}\left[\frac{K_X^{\circ} + [X]}{K_X^{\circ} + Q_{AX}[X]}\right] \quad (3)$$

$$K_A = K_A^{\circ}\left[\frac{K_Y^{\circ}[X] + K_X^{\circ}[Y] + Q_{XY}[X][Y] + K_X^{\circ}K_Y^{\circ}}{K_Y^{\circ}Q_{AX}[X] + K_X^{\circ}Q_{AY}[Y] + Q_{AXY}[X][Y] + K_X^{\circ}K_Y^{\circ}}\right] \quad (4)$$

$$K_A^{\circ\prime} = K_A^{\circ}\left[\frac{K_Y^{\circ} + [Y]}{K_Y^{\circ} + Q_{AY}[Y]}\right] \quad (5)$$

$$K_X^{\circ\prime} = K_X^{\circ}\left[\frac{K_Y^{\circ} + [Y]}{K_Y^{\circ} + Q_{XY}[Y]}\right] \quad (6)$$

$$Q_{AX}' = \left[\frac{(K_Y^{\circ} + [Y])(K_Y^{\circ}Q_{AX} + Q_{AXY}[Y])}{(K_Y^{\circ} + Q_{AY}[Y])(K_Y^{\circ} + Q_{XY}[Y])}\right] \quad (7)$$

The parameters have the following definitions: A = substrate (PEP), X = allosteric ligand (FDP), Y = allosteric ligand (Mn^{2+}), K_A = concentration of substrate A producing half-maximum velocity, $K_A^{\circ} = K_A$ when [X] = [Y] = 0, K_X° = dissociation constant of X when [A] = [Y] = 0, K_Y° = dissociation constant of Y when [A] = [X] = 0, Q_{AX} = coupling parameter between bound A (PEP) and bound X (FDP), Q_{AY} = coupling parameter between bound A (PEP) and bound Y (Mn^{2+}), Q_{XY} = coupling parameter between bound X (FDP) and bound Y (Mn^{2+}), and Q_{AXY} = coupling parameter between bound A (PEP), bound X (FDP), and bound Y (Mn^{2+}). The coupling parameters describe the influence that the binding of one of the indicated ligands has on the binding of the other ligand. They are related to the corresponding free energy of interaction, or the coupling free energy, between the indicated ligands according to the expression (Reinhart, 1983)

$$\Delta G_{AX} = -RT \ln Q_{AX} \quad (8)$$

where R equals the gas constant and T equals the absolute temperature. Thus, if $Q_{AX} = 1$, then $\Delta G_{AX} = 0$, and no interaction exists between ligands A and X on the enzyme and they bind independently. If $Q_{AX} < 1$, then $\Delta G_{AX} > 0$, and the binding interaction is "negative", indicating that the binding of X antagonizes the binding of A. If $Q_{AX} > 1$, then $\Delta G_{AX} < 0$, indicating a "positive" interaction since the binding of X increases the affinity of the enzyme for A. It follows that the coupling free energy for the simultaneous binding of all three ligands is given by $\Delta G_{AXY} = -RT \ln Q_{AXY}$. This coupling free energy is the difference between the free energy of binding of all three ligands simultaneously and the sum of the individual binding energies for each ligand binding to the enzyme separately [see Reinhart (1983, 1988)]. A prime (′) on a parameter designates that it is "apparent".

Data were fit by either the nonlinear least-squares fitting program, EZ-FIT (Perella, 1988), or Table Curve 3D (Jandel Scientific) on an IBM compatible 80386 computer equipped with a math coprocessor. The error in the fitted parameters is shown as error bars in graphs and was used as weighting factors in model fitting. The weighting factor used was 1/(error in parameter)^2. Precision in individual velocity determinations was typically within 3%.

RESULTS

Influence of Mn^{2+} on the Velocity of the YPK-Catalyzed Reaction. The steady-state kinetic response of YPK to varying concentrations of PEP, FDP, and free Mn^{2+} is illustrated in Figure 1. These data were obtained at pH 6.2 and at free Mn^{2+} concentrations as indicated. The concentrations of free Mn^{2+} were calculated primarily for binding to ADP. A number of effects is apparent from the velocity profiles in Figure 1. First, YPK behaves as a classical "K-type" enzyme system since the maximal velocity obtained at saturating PEP, in the presence and absence of FDP, and at varying concentrations of Mn^{2+}, is approximately 65 ± 10 units/mg. The 80−90 units obtained at 29 μM Mn^{2+} is higher because the enzyme used for this study was from a different YPK purification. In other studies, using YPK from a single enzyme purification, V_{max} values also indicate a "K-type" activation. Since the simultaneous binding of PEP, FDP, and Mn^{2+} with YPK has little or no effect on V_{max}, it is convenient to express the allosteric activation of YPK with eqs 3−7 (Reinhart, 1985).

Second, the binding of Mn^{2+} to YPK affects both the sigmoidal nature of the response of YPK to both FDP and PEP and the concentration of FDP and PEP required to produce half-maximal activity. Thus, data in both the PEP and FDP dimension were fit to eqs 1 and 2. In the FDP dimension, the initial velocity v was corrected by subtracting the velocity in the absence of FDP, v_o. Equation 2 fit the data best in both dimensions over most of the concentration ranges studied. With increasing FDP concentrations, both equations fit the data equally well since the Hill coefficients of PEP approach values of 1. At high PEP concentrations, the data for FDP could not be fit to either equation since the difference between v and v_o values approach zero as V_{max} is obtained. The apparent Michaelis constants for PEP, Mn^{2+}, and FDP, obtained at saturating levels of the fixed variable ligand(s), were calculated by use of either eq 1 or 2 as appropriate. The apparent Michaelis constants and the associated Hill coefficients for these ligands are summarized in Table 1.

[3] For a more complete description of the derivation of these equations and their use in quantifying allosteric kinetic parameters, see Reinhart (1983, 1985, and 1988).

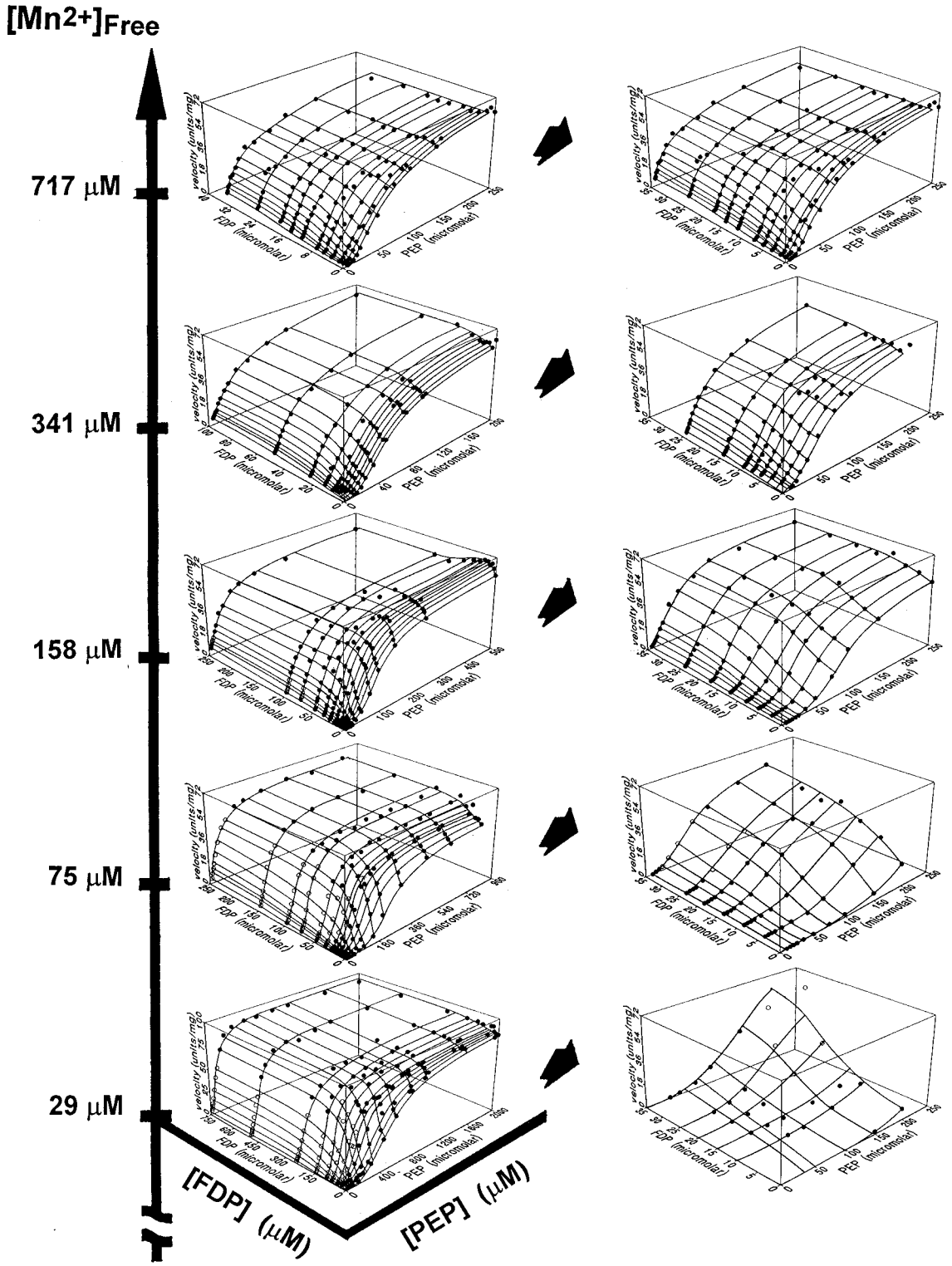

FIGURE 1: Fourth-dimensional plot of the steady-state kinetic rate profiles for YPK as a function of PEP, FDP, and Mn^{2+} concentrations. The concentration of PEP was varied at fixed, variable FDP concentrations, and the total Mn^{2+} concentration was held constant. Open circles represent initial velocity data calculated from the linear, steady-state portion of progress curve data that had an associated lag phase. The 3-D plots on the left side of the arrows were blown up in order to more clearly illustrate the effect of Mn^{2+} on the curvature of the kinetic profiles. These plots are shown on the right side of the arrows, and the concentration ranges for PEP and FDP are equal in each plot with PEP ranging from 0 to 250 μM and FDP ranging from 0 to 35 μM. The velocity range of each plot ranges from 0 to 72 units/mg. Starting with the lower, left-hand 3-D plot and then moving up the $[Mn^{2+}]_{free}$ axis: total Mn^{2+} is 1 mM and free Mn^{2+} is 29 μM, PEP was varied from 10 to 2000 μM, FDP was varied from 0 to 750 μM, and lag times ranged from approximately 10 to 250 s; total Mn^{2+} is 2 mM and free Mn^{2+} is 75 μM, PEP was varied from 10 to 800 μM, FDP was varied from 0 to 250 μM, and lag times ranged from approximately 10 to 45 s; total Mn^{2+} is 3 mM and free Mn^{2+} is 158 μM, PEP was varied from 6 to 500 μM, FDP was varied from 0 to 250 μM, and lag times ranged from approximately 10 to 20 s; total Mn^{2+} is 4 mM and free Mn^{2+} is 341 μM, PEP was varied from 5 to 200 μM, FDP was varied from 0 to 2000 μM, and data from 100 to 2000 μM FDP was omitted in order to show the curvature at lower FDP concentrations; lag phases were not observed in progress curves; total Mn^{2+} is 5 mM and free Mn^{2+} is 717 μM, PEP was varied from 5 to 250 μM, FDP was varied from 0 to 100 μM, and data from 40 to 100 μM FDP was omitted in order to show the curvature at lower FDP concentrations. Lag phases were not observed in progress curves.

Table 1: Kinetic Constants of PEP and the Activators[a]

ligand	activator[b]	K_M (μM)	n_H
PEP	(−) FDP	56 ± 2	2.3 ± 0.1
	(+) FDP	21 ± 3	1
free Mn^{2+}	(−) FDP	15 ± 1	2.0 ± 0.3
	(+) FDP	8.0 ± 0.5	1
FDP		7.8 ± 1.8	1.4 ± 0.4

[a] The kinetic constants were calculated from either eq 1 or eq 2 as appropriate as determined at saturating concentrations of the two fixed variable ligands. The V_{max} value for these experiments is 65 units/mg. The same V_{max} value is measured in the presence or absence of FDP defining YPK as a K-type system. [b] The activator is defined as the heterotropic activator FDP.

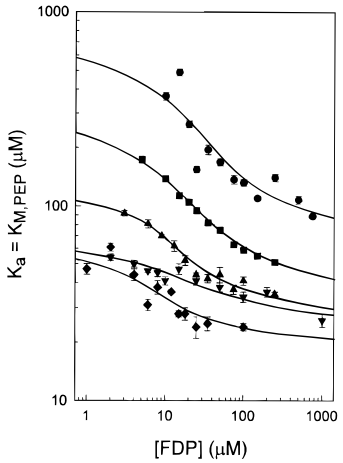

FIGURE 2: Influence of Mn^{2+} on the FDP dependence of the apparent Michaelis constant, K_A, for PEP. The points represent apparent $K_A°$ values determined from fitting the steady-state velocity data to eq 2. Error bars represent the error in the fit of the data to eq 2 for each individual point. The curves represent the best-fit of the data for each Mn^{2+} concentration to eq 3. Free Mn^{2+} concentrations are 29 μM (●), 75 μM (■), 158 μM (▲), 341 μM (▼), and 717 μM (◆).

Finally, Mn^{2+} affects the shapes of the YPK reaction progress curves. The open symbols in Figure 1 represent velocity data that was obtained from the final, fast and linear phases of the progress curves. The data represent only the steady-state velocity of the activated enzyme species. Lag phases are observed at low Mn^{2+} concentrations and are dependent on the concentration of the various ligands. They ranged from 10 to 250 s with the longer times occurring at lower Mn^{2+} concentrations. Analysis of the data in Figure 1 indicates that PEP is more effective than FDP in diminishing the lag times, as judged by the lower concentration of PEP, relative to its K_M value, necessary to eliminate the lag phase. The substrate and activator concentration dependent elimination of the lag phases suggest that yeast PK maybe a "hysteretic" enzyme, similar to that of human erythrocyte PK (Badwey & Westhead, 1976). Including hysteretic mechanisms in our analysis was unnecessary since the velocities measured were steady-state velocities (Badwey & Westhead, 1976; Reinhart, 1983; Symcox & Reinhart, 1992).

Influence of Mn^{2+} on the Steady-State Kinetic Parameters of YPK. The influence of Mn^{2+} on the apparent Michaelis constants for PEP (K_A) as a function of FDP is shown in Figure 2. Increasing the FDP concentration decreases the apparent $K_A°$ for PEP until a plateau is reached. This behavior is characteristic of allosteric activation in which two ligands bind simultaneously to an enzyme (Reinhart, 1983) and is described by eq 3. Thus, the data at each Mn^{2+} concentration in Figure 2 was best-fit to eq 3 and appears to be well described by this model. The change in shapes of the curves in Figure 2 indicates that Mn^{2+} influences all three of the apparent kinetic parameters (Reinhart, 1985): Q_{AX}, the coupling parameter between bound PEP and bound FDP; $K_A°$, the apparent dissociation constant of PEP when [FDP] = 0; and $K_X°$ the apparent dissociation constant of FDP when [PEP] = 0. The resulting values for these apparent kinetic parameters are summarized in Table 2.

Table 2: Apparent Allosteric Kinetic Parameters for the Data in Figure 2 as Fit to Eq 3[a]

$[Mn^{2+}]_{free}$ (μM)	$K_A°'$ (PEP) (μM)	$K_X°'$ (FDP) (μM)	$Q_{AX}°'$
29	548 ± 18	81 ± 18	6.4 ± 0.7
75	245 ± 2	49 ± 3	5.7 ± 0.1
158	103 ± 4	33 ± 10	3.5 ± 0.4
341	58 ± 3	20 ± 8	1.9 ± 0.2
717	58 ± 5	19 ± 14	3.1 ± 0.8

[a] The prime (′) indicates that the values for these parameters are apparent values.

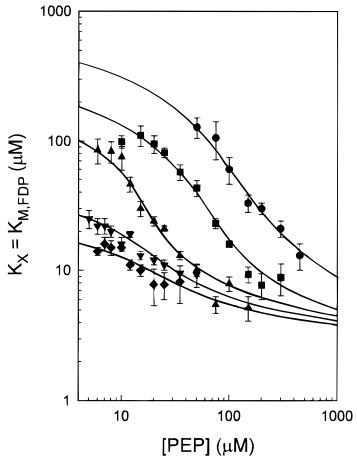

FIGURE 3: Influence of Mn^{2+} on the dependence of the apparent Michaelis constant, K_X, for FDP on [PEP]. The points represent apparent $K_X°$ values determined from fitting the steady-state velocity data to eq 2. Error bars represent the error in the fit of the data to eq 2 for each individual point. The curves are drawn to show the general trend of the data at each Mn^{2+} concentration. Free Mn^{2+} concentrations are 29 μM (●), 75 μM (■), 158 μM (▲), 341 μM (▼), and 717 μM (◆).

The kinetic parameters in Table 2 show that in the presence of FDP, increasing the concentration of Mn^{2+} decreases the apparent $K_A°$ of PEP. In addition, increasing the concentration of Mn^{2+} lowers the apparent $K_X°$ of FDP at low and high concentrations of PEP, indicating that Mn^{2+} influences the binding of both PEP and FDP. The mutual effect of Mn^{2+} and FDP on the apparent K_M of PEP, and the effect of Mn^{2+} and PEP on the apparent K_M of FDP, is predicted by thermodynamic linkage (Weber, 1975).

The curves in Figure 3 were plotted to represent the trend in the data. A best-fit of the data to eq 3 was not obtained because the algorithms used were unable to converge to a single, well-defined minimum. The trends in the data shown in Figures 2 and 3 appear to be the same. Both sets of data indicate that the values for the apparent Michaelis constants for PEP and FDP decrease as Mn^{2+} increases. The magnitudes of Q_{AX} as a function of Mn^{2+} for both data sets also appear to be similar and verifies the rapid-equilibrium assumption as proposed by Symcox and Reinhart (1992).

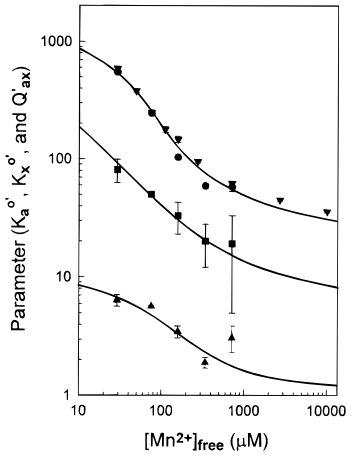

FIGURE 4: Influence of Mn^{2+} on the parameters describing the allosteric activation of YPK by PEP and FDP. The apparent parameters $K_A^{o\prime}$ (●), $K_X^{o\prime}$ (■), and Q_{AX}' (▲) were determined by fitting the data in Figure 2 to eq 3. $K_A^{o\prime}$ (▼) was also determined from fitting the data in Figure 5 to eq 2. The curves represent plots of eqs 5−7 using values shown in Table 3.

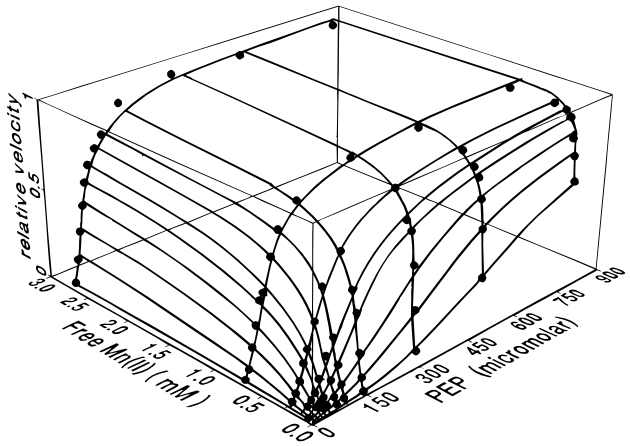

FIGURE 5: Steady-state kinetic rate profile for YPK as a function of PEP and Mn^{2+}. The concentration of PEP was varied at different fixed, variable total Mn^{2+} concentrations. Free Mn^{2+} concentrations were calculated. In each plot, the curves in both dimensions represent the best-fit of the data to eq 2 as described in the text.

Their argument states that the ratio of the apparent dissociation constants for the allosteric ligand at limiting and saturating substrate concentrations yields the true thermodynamic coupling parameter Q_{AX} between the allosteric ligand and the substrate. This relationship is true even in the steady-state case. The method further explains that if the value of Q_{AX} measured by the approach indicated above is the same as the value of Q_{AX} measured from the ratio of the Michaelis constants for the substrate in the absence and saturating presence of the allosteric effector, then the substrate may be considered as achieving a binding equilibrium in the steady-state. Thus, the equivalence of Q_{AX} values determined from both K_A and K_X data validates the rapid-equilibrium assumption for the YPK system and implies that at least one of the ligands, PEP or FDP, is achieving binding equilibrium in the steady-state.

Direct binding studies of FDP to the YPK−PEP−Mn^{2+} complex indicate that the dissociation constant for FDP from this complex is equivalent to the Michaelis constant for FDP measured by kinetic studies (Mesecar & Nowak, 1997a,b). The equivalence of K_D and K_M for FDP indicates that FDP is achieving a rapid equilibrium in the steady-state. Thus, the utility of eq 4 for analyzing the influence of the apparent Michaelis constants of PEP as a function of Mn^{2+} and FDP is justified, and it is therefore necessary only to analyze the data in Figure 2 to obtain the additional allosteric parameters needed to describe the ligand interactions involved in the formation of the YPK−PEP−FDP−Mn^{2+} complex.

The apparent kinetic parameters $K_A^{o\prime}$, $K_X^{o\prime}$, and Q_{AX}' listed in Table 2 are shown plotted as a function of Mn^{2+} concentration in Figure 4. Equations 5−7 describe the influence of these parameters by a third ligand Y or Mn^{2+}. In order to fit the entire data set in Figure 4 to these equations, an initial fit of $K_A^{o\prime}$ to eq 5 is obtained first for the assessment of $K_X^{o\prime}$. Initial attempts of fitting the data for $K_A^{o\prime}$ to eq 5 were unsuccessful due to an insufficient amount of data, primarily at the extremes of low and high Mn^{2+} concentrations.

The interactions of PEP and Mn^{2+} with YPK were studied by steady-state kinetics in the absence of FDP to increase the number of $K_A^{o\prime}$ data points in Figure 4. Figure 5 shows the results of the steady-state rate profile for varying PEP concentrations at fixed variable Mn^{2+} concentrations. PEP concentrations ranged from 20 to 800 μM and free Mn^{2+} concentrations ranged from 29 μM to 10 mM. The data in both dimensions was best-fit to eq 2 over the entire concentration range studied. Equation 1 failed to accurately fit the data in all cases.

Influence of Free ADP on the Binding of PEP. Attempts to measure $K_A^{o\prime}$ values for PEP below 29 μM free Mn^{2+} were difficult because of decreasing concentrations of MnADP and increasing concentrations of free ADP when total ADP is fixed. Approximately 1 mM MnADP is required to saturate YPK. The steady-state velocity profile for the interaction of PEP with YPK at 10 μM free Mn^{2+}, 1 mM MnADP, and 13 mM free ADP was measured (data not shown). A K_M value of 3.5 ± 0.07 mM and a n_H value of 3.8 ± 0.02 for PEP results from a fit of the data to eq 2. The K_M or $K_A^{o\prime}$ value for PEP is higher than the dissociation constant of 1.6 ± 0.05 mM for PEP from the YPK−PEP complex determined from steady-state fluorescence titration data (vide infra Figure 6). This discrepancy may result from several factors (see Discussion).

The dissociation constant for PEP binding to the YPK−ADP complex was measured in order to determine if the high levels of free ADP associated with kinetic studies at low free Mn^{2+} influence the interaction of PEP with YPK. The results in Figure 6 show that saturating levels of free ADP decrease the affinity of YPK for PEP by approximately 5-fold, indicating that free ADP antagonizes the binding of PEP. Thus, at low free Mn^{2+} concentrations, an increase in the apparent $K_A^{o\prime}$ values of PEP above its K_D is attributable to high levels of free ADP that antagonize PEP binding.

To fully describe the kinetic properties of yeast pyruvate kinase, the binding of free ADP to YPK should be taken into account. This task becomes exceedingly difficult when one considers that a single monomer of YPK must form a complex with at least five ligands (free Mn^{2+}, MnADP, PEP, H^+, and K^+) in order for catalysis to occur. The inclusion of FDP and free ADP into the rate equation increases the number of ligands bound to seven, further complicating the analysis. The fact also remains that YPK is a tetramer with the existence of heterotropic and homotropic interactions between a number of these ligands, making a difficult task arduous. By keeping the concentrations of MnADP, H^+, and

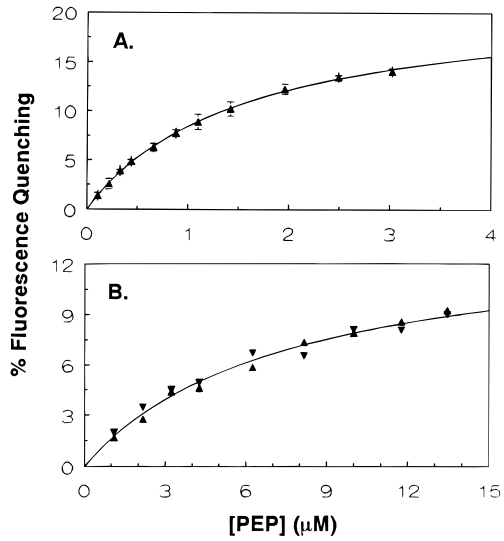

FIGURE 6: The binding of PEP to various yeast pyruvate kinase complexes measured by intrinsic tryptophan fluorescence quenching. The amount of fluorescence quenching was calculated as described in the Experimental Procedures. (A) PEP titration of free YPK. The points represent the average of three sets of experiments, and the error bars represent the standard deviation. The curve represents the best-fit of the data to a simple binding isotherm equation as cooperativity of PEP binding was not observed. The resulting dissociation constant for PEP to YPK is 1.57 ± 0.05 mM, and the percent maximal quenching value Q_M is 21.6 ± 0.4%. (B) PEP titration of the YPK−ADP binary complex. The concentration of ADP in the titration mixture was 9.1 mM. The points are the results of two separate experiments. The curve represents the best-fit of the data to a simple binding isotherm equation as cooperativity of PEP binding was not observed. The resulting dissociation constant for PEP to the YPK−ADP binary complex is 7.7 ± 0.8 mM and the percent maximal quenching value Q_M is 14.0 ± 0.7%.

K^+ fixed and by minimizing the concentration of free ADP by restricting the free Mn^{2+} concentrations to above 29 μM, the rate equation can be simplified to include the interactions of just three ligands, free Mn^{2+}, PEP, and FDP. Since YPK is a K-type system and because the allosteric effector is in rapid equilibrium as shown above, the allosteric coupling parameters between the various ligands in the YPK−PEP−FDP−Mn^{2+} complex can be quantified using eqs 5−7.

Calculation of Heterotropic Kinetic Coupling Parameters. The apparent $K_A°'$ values for PEP obtained from Figure 5 are shown plotted as a function of Mn^{2+} within Figure 4. The experimentally measured values of $K_A°'$ for PEP in the absence FDP coincide with the $K_A°'$ values calculated from eq 3 for the data obtained in the presence of FDP (Figure 2). These are the expected results if eq 3 accurately represents the data. The entire $K_A°'$ data set was then fit to eq 5. The calculated value of $K_Y°$ (880 μM), the apparent dissociation constant of Mn^{2+} to the free enzyme, was placed into eq 6 to fit the $K_X°$ data. The resulting parameters, $K_Y°$ = 880 μM, Q_{AY} = 105, $K_X°$ = 129 μM, and Q_{XY} = 20, obtained from eqs 5 and 6, were then used with eq 7 to fit the Q_{AX}' data. The algorithm could not converge to a local minimum when fitting data to eq 7 with Q_{AX} as a floating point parameter. Therefore, Q_{AX} was fixed at different values ranging from 30 to 0.001 allowing the algorithm to converge. The resulting values of Q_{AXY} and the associated errors are shown in Table 3.

The errors in Q_{AXY} as a function of Q_{AX} suggest that a Q_{AX} value of 1 would best describe the data. Although values of Q_{AX} less than 1 have slightly lower errors, the corresponding free energy of interaction between FDP and PEP would be large and positive, implying an antagonistic relationship between the two ligands. A Q_{AX} value of 1, however, suggests that FDP and PEP bind to the enzyme simultaneously and independently, a more likely situation considering the data in Figures 2 and 3. Thus, the Q_{AX}' values in Figure 4 were fit to eq 7, with Q_{AX} fixed at a value of 1. The resulting best-fit curves to eqs 5−7 are shown in Figure 4 and the values for parameters obtained from these fits are summarized in Table 4.

Since eq 4 describes the expected behavior of the K_A of PEP as a function of the two allosteric ligands, FDP and Mn^{2+}, a global fit of the data in Figure 2 to eq 4 was performed. In addition, the K_A values for PEP in the absence of FDP obtained from Figure 4 were merged with this data set. The resulting best-fit surface is shown in Figure 7, and the kinetic parameters that define this surface are listed in

Table 3: Fluctuation of Q_{AXY} Values as a Result of Fixing Q_{AX} Values in Eq 7[a]

fixed value of Q_{AX}	coupling free energy ΔG_{AX}[b] (kcal/mol)	value of Q_{AXY} from eq 10	% error
30	−2.0	658 ± 289	43.9
10	−1.4	1086 ± 192	17.7
4	−0.8	1214 ± 166	13.7
2	−0.4	1256 ± 158	12.6
1	0	1277 ± 154	12.1
0.9	0.06	1278 ± 154	12.0
0.1	1.4	1297 ± 150	11.6
0.01	2.7	1299 ± 150	11.6
0.001	4.0	1299 ± 150	11.6

[a] The program EZ-FIT was used to calculate the values for Q_{AXY} at different fixed values for Q_{AX}. A weighting function of $1/(\Delta Q_{AX}')^2$ was introduced into each nonlinear regression calculation. $\Delta Q_{AX}'$ represents the error in Q_{AX}' calculated from the fit of the data in Figure 2 to eq 3. [b] Coupling free energies were calculated according to eq 8 with T = 24 °C.

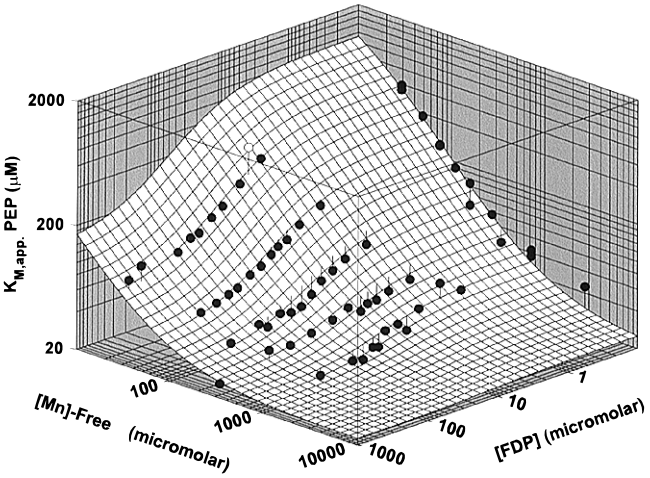

FIGURE 7: Influence of FDP and Mn^{2+} on the apparent Michaelis constant, $K_A°$, for PEP. The values for $K_A°'$ are the same values plotted in Figure 2. The surface is the best-fit surface of the data to eq 4 and was calculated using the program Table Curve 3D (Jandel Scientific). The unfilled circle represents a point not included in the calculations. The initial parameter estimates were determined from fits to eqs 5−7 (see Table 3). A weighting function of $1/(\Delta K_A°')^2$ was introduced into each nonlinear regression calculation. $\Delta K_A°'$ is the calculated error in the fits from fitting the steady-state rate data to eq 2. The r^2 coefficient of determination was 0.9908, and the degrees of freedom adjusted coefficient of determination was 0.9897. The resulting kinetic parameters from this fit are shown in Table 4.

Table 4: Steady-State Allosteric Kinetic Parameters Describing the Combined Influence of FDP and Mn^{2+} on the Apparent Michaelis Constant for PEP[a]

parameter	eqs 5−7[b]	eq 4[c]
$K_A°$ (μM)	2466 ± 1352	2440 ± 541
$K_X°$ (μM)	129 ± 15	150 ± 56
$K_Y°$ (μM)	880 ± 685	860 ± 333
Q_{AX}	1[d]	1.0[d]
ΔG_{AX} (kcal/mol)	0	0
Q_{AY}	105 ± 56	105 ± 25
ΔG_{AY} (kcal/mol)	−2.75 ± 0.36	−2.75 ± 0.14
Q_{XY}	20 ± 4	14 ± 14
ΔG_{XY} (kcal/mol)	−1.77 ± 0.12	−1.55 ± 1.03
Q_{AXY}	1278 ± 154	1520 ± 880
ΔG_{AXY} (kcal/mol)	−4.22 ± 0.07	−4.32 ± 0.40

[a] A = PEP, X = FDP, and Y = Mn^{2+}. Coupling free energies were calculated according to eq 8 with T = 24 °C. [b] The program EZ-FIT was used to fit eqs 5−7 to the apparent parameters in Figure 4. A weighting function of $1/(\Delta p)^2$ was introduced into each nonlinear regression calculation. Δp is the standard error in the apparent parameters determined from the best-fit curves of the data in Figure 2 to eq 3. [c] The program Table Curve 3D was used to fit eq 4 to the apparent $K_A°'$ values in Figure 2. The resulting best-fit surface is shown in Figure 7. [d] The value of Q_{AX} was fixed at 1 for these calculations (see text).

Table 4. The choice of starting parameters for eq 4 was critical for convergence of the algorithm. The starting parameters chosen and the parameters that led to the best-fit surface were those obtained from fitting the apparent parameter values to eqs 5−7. Note that the value of 0 kcal/mol for the PEP−FDP coupling free energy results from fixing Q_{AX} at a value of 1 in eqs 4 and 7. The choice of a value of 1 is justified for the following reasons.

First, the results of error analysis in Table 3 indicate that as Q_{AX} values approach values of 1 and below, the error in the Q_{AXY} reaches a minimum plateau. As Q_{AX} values approach 0, the coupling free energy between PEP and FDP approaches infinity. A Q_{AX} value of zero indicates that the binding of PEP and FDP is mutually exclusive. Furthermore, the implication that a model must provide for $Q_{AX} = 0$ ($\Delta G_{AX} = \infty$) must also allow for $Q_{AXY} = 0$ by the relationship $Q_{AXY} = Q_{AX}Q_{AY}Q_{XY/A}$. Accordingly, the equation describing the expected behavior of the apparent Michaelis constant for PEP when FDP and PEP are mutually exclusive can be derived from eq 4 by setting Q_{AX} and $Q_{AXY} = 0$. The resulting equation is:

$$K_A = K_A°\left[\frac{K_Y°[X] + K_X°[Y] + Q_{XY}[X][Y] + K_X°K_Y°}{K_X°Q_{AY}[Y] + K_X°K_Y°}\right] \quad (9)$$

Numerous attempts to fit the data in Figure 7 to eq 9 were made, but the algorithm could not converge to a local minimum regardless of the choices for the starting parameters. Simulations of surface plots of eqs 4 and 9, using the parameters determined from eqs 5−7, indicate that the Q_{AXY} term must be included in order to describe the data (plots not shown). Therefore, the value for Q_{AX} must be finite and included in the model.

Second, the kinetically derived value for ΔG_{AX} is close to the thermodynamically determined value of ΔG_{AX} (−0.22 kcal/mol), obtained by direct binding studies [see Table 5 and Mesecar and Nowak (1997a)]. The results of both kinetic and thermodynamic studies indicate that there is little free energy of interaction between FDP and PEP.

Table 5: Comparison of the Allosteric Parameters for Yeast Pyruvate Kinase Determined from Two Different Methods[a]

parameter	kinetically derived values	thermodynamically derived values
K_{PEP}^0 (μM)	2440 ± 540	1106 ± 187
K_{FDP}^0 (μM)	150 ± 56	321 ± 7
K_{Mn}^0 (μM)	860 ± 333	7160 ± 930
$\Delta G_{PEP-FDP}$ (kcal/mol)	0	−0.22 ± 0.03
ΔG_{Mn-PEP} (kcal/mol)	−2.75 ± 0.14	−3.88 ± 0.08
ΔG_{Mn-FDP} (kcal/mol)	−1.55 ± 1.03	−1.09 ± 0.02
$\Delta G_{Mn-PEP-FDP}$ (kcal/mol)	−4.32 ± 0.40	−6.60 ± 0.09

[a] The kinetically derived values were determined from this study. The thermodynamically derived values were obtained from direct binding studies described in the following paper (Mesecar & Nowak, 1997a).

The utility of eq 4 in describing the data for the heterotropic interactions of PEP, FDP, and Mn^{2+} with YPK is obvious from the fitted surface plotted in Figure 7. The degrees-of-freedom (DOF) adjusted r^2 coefficient of determination for the resulting surface fit was 0.9897. This is a coefficient of determination that has been adjusted for the degrees-of-freedom in eq 4. The standard r^2 value will increase as a direct result of increasing the number of terms in an equation even though there has been no real improvement in the standard error of the fit. The DOF adjusted r^2 better represents the true least-squares r^2 best-fit criteria, and the closer this value is to 1.0, the better the statistical measure of fit. Thus, eq 4 provides a good, statistically sound and global-fit to the data presented in Figure 7. A comparison of the parameters in Table 4 suggests that both fitting methods lead to essentially the same values for the steady-state kinetic parameters.

Homotropic Responses of YPK to PEP, FDP, and Mn^{2+}. The coupling parameters given in Table 4 indicate that positive, heterotropic cooperative interactions exist between PEP, FDP and Mn^{2+}, and YPK. The sigmoidal nature of the velocity profiles in Figures 1 and 5 indicates that homotropic cooperative interactions also exist with these ligands in addition to the heterotropic interactions. Presently, the collective homotropic interactions of PEP, FDP, and Mn^{2+} with YPK described in these studies cannot be quantified. A theoretical model with pertinent mathematical descriptions for a homotropic, three ligand system with heterotropic interactions has not yet been developed. A qualitative model can be formulated from the data presented however.

The magnitude and nature of homotropic cooperativity is related to the value of the Hill coefficient, n_H, from eq 2. The Hill coefficient represents an average site−site coupling constant (e.g., Q_{AA}, Q_{XX}, or Q_{YY}) and reflects both the oligomeric state of the protein as well as the magnitude of the free energy of interaction between each of the sites.[4] In the case of a homotetramer such as YPK and assuming the absence of any substantial monomer/dimer/tetramer equilibrium and the absence of asymmetric communication between sites, *some* of the homotropic coupling parameters involved would be: Q_{AA}, Q_{AAA}, Q_{AAAA}, Q_{XX}, Q_{XXX}, Q_{XXXX}, Q_{YY}, Q_{YYY}, and Q_{YYYY}, representing site−site coupling in

[4] The mathematical relationship between the Hill coefficient (n_H) and the homotropic coupling constant Q_{AA}, and hence ΔG_{AA}, for a dimer and tetramer is described by Reinhart (1988) and Johnson and Reinhart (1993).

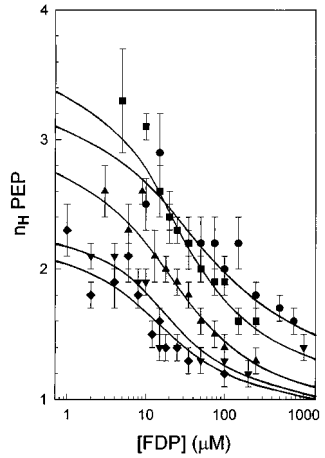

FIGURE 8: Influence of the Hill coefficient (n_H) for PEP by FDP and Mn^{2+}. The values of n_H were determined from fitting the steady-state velocity data in Figure 1 to eq 2. Error bars represent the error in the fit of the data to eq 2 for each individual point. The curves are drawn to show the general trend of the data at each Mn^{2+} concentration. Free Mn^{2+} concentrations are 29 μM (●), 75 μM (■), 158 μM (▲), 341 μM (▼), and 717 μM (◆).

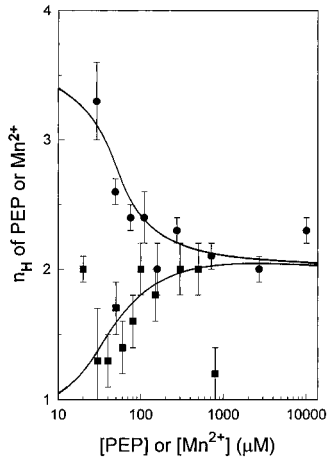

FIGURE 9: Influence of the Hill coefficients (n_H) for PEP and Mn^{2+} in the absence of FDP. The values of n_H were determined from fitting the steady-state velocity data in Figure 5 to eq 2. Error bars represent the error in the fit of the data to eq 2 for each individual point. The curves represent the general trend of the data. The n_H values for PEP are plotted as a function of Mn^{2+} (●), and the n_H values for Mn^{2+} are shown plotted as a function of PEP (■).

the absence of any other ligand(s), and $Q_{AA/XX}$, $Q_{AAA/X}$, $Q_{AAAA/XXY}$, $Q_{XX/AA}$, $Q_{XXX/YYY}$, $Q_{XXXX/AAYY}$, $Q_{YY/AAXX}$, $Q_{YYY/A}$, and $Q_{YYYY/AAAAXXXX}$ etc., representing site−site coupling in the presence of other ligand(s). The number of letters in the subscripts before the slash (/) indicates the number of occupied and communicating sites. The number of subscripts after the slash represents the degree of saturation at the other sites. Because of the complexity and the number of interactions possible, it is more convenient to simplify the analysis by describing only the "average" site−site coupling parameters Q_{AA}, Q_{XX}, and Q_{YY} for ligands A, X, or Y. It follows that if the binding of the first ligand lowers the dissociation constant for the binding of a second ligand, then $n_H > 1$, $\Delta G_{AA} < 0$ and "positive" cooperativity occurs. If the binding of the first ligand raises the dissociation constant for the binding of a second ligand, then $n_H < 1$, $\Delta G_{AA} > 1$ and "negative" cooperativity occurs. No interaction between sites exists when $n_H = 1$, since $\Delta G_{AA} = 0$. Thus, the magnitude of the Hill coefficients may be used to describe the extent and nature of the homotropic interactions occurring on the enzyme.

A plot of the Hill coefficient for PEP as a function of FDP and Mn^{2+} is shown in Figure 8. The data indicate that increasing the concentration of Mn^{2+} at low FDP concentrations lowers the amount of positive homotropic coupling since n_H decreases from approximately 3.5 to 2. Increasing the concentration of Mn^{2+} at higher concentrations of FDP abolishes the amount of positive homotropic cooperativity since n_H values approach 1. The data also suggest that increasing the concentration of FDP at low Mn^{2+} does not abolish the positive cooperativity in PEP binding since n_H approaches values of 1.4. However, the addition of Mn^{2+} to the FDP saturated enzyme abolishes PEP positive cooperativity. The relative magnitudes for the coupling parameters derived from this data are then $\sim 10 > Q_{AA/XY} > Q_{AA/XYY} \geq Q_{AA/XXY} > 1$ and $Q_{AA/XXYY} = 1$ giving coupling free energies of ~ -1.4 kcal/mol $< \Delta G_{AA/XY} < \Delta G_{AA/XYY} \leq \Delta G_{AA/XXY} < 0$ kcal/mol and $\Delta G_{AA/XXYY} = 0$ kcal/mol, respectively.[4]

The Hill coefficients for PEP are plotted against the concentration of Mn^{2+} in the absence of FDP in Figure 9. The value of n_H for PEP decreases from a value of about 3.4 at low Mn^{2+} to a value of 2 at high Mn^{2+}, indicating that the binding of PEP is positively cooperative over the entire concentration range of Mn^{2+} studied. The results of direct binding studies, however, show that the interaction of PEP with YPK in the absence of Mn^{2+} exhibits no cooperativity since n_H for PEP is 1 (Figure 6). Therefore, the coupling parameter for PEP in the absence of additional ligands (Q_{AA}) is 1 and $\Delta G_{AA} = 0$. In the presence of Mn^{2+}, the coupling parameter $Q_{AA/YY}$ approaches a value of ~ 2.5 making $\Delta G_{AA/YY} \approx -0.6$ kcal/mol. Thus, Mn^{2+} heterotropically induces positive homotropic cooperativity in PEP binding. The response of YPK to the binding of PEP once again becomes hyperbolic in the saturating presence of both Mn^{2+} and FDP ($Q_{AA/XXYY} = 1$ and $\Delta G_{AA/XY} = 0$), indicating that FDP heterotropically abolishes cooperative binding of PEP.

The Hill coefficients for Mn^{2+} are also plotted in Figure 9 against the concentration of PEP. The values of n_H for Mn^{2+} increase from values near 1 at low concentrations of PEP to values approaching 2 at higher concentrations of PEP. The trend in the n_H data for Mn^{2+} suggests that PEP induces homotropic cooperativity in Mn^{2+} activation. In addition, the response of YPK once again becomes hyperbolic upon saturation with FDP, indicating that FDP heterotropically abolishes the positive cooperativity in Mn^{2+} binding (Table 1). The trend in the homotropic response of YPK to Mn^{2+} is analogous to its response to PEP. As a result, $Q_{YY} = Q_{YY/AAXX} = 1$ and $Q_{YY/AA} \approx 2.5$, making $\Delta G_{YY} = \Delta G_{YY/AX} = 0$ and $\Delta G_{YY/AA} \approx -0.6$ kcal/mol, respectively.

Trends in the Hill coefficients for FDP as a function of PEP or Mn^{2+} are not described because of the associated errors in the values of n_H for FDP. However, most of the values for n_H were greater than 1 and less than 3, indicating that homotropic cooperativity of FDP binding is observable under a wide range of experimental conditions (data not shown). Interestingly, saturation of the enzyme with both additional ligands does not abolish the positive cooperative binding of FDP ($Q_{XX/AAYY} > 1$, Table 1), in contrast to the situation with PEP and Mn^{2+} where $Q_{AA/XXYY} = Q_{YY/AAXX} = 1$. These observations are consistent with the values of

n_H obtained for FDP from direct binding studies (Mesecar & Nowak, 1997a).

DISCUSSION

Manganese(II) activated yeast pyruvate kinase behaves as a classical K-type allosteric enzyme as defined by Monod et al. (1965). Magnesium(II) activated yeast pyruvate kinase also acts a K-type activator system with FDP (Hunsley & Suelter, 1969; Morris et al., 1986; Ford & Robinson, 1976; Johannes & Hess, 1973). The effects of Mg^{2+} and Mn^{2+} on the interactions of ligands to YPK appear similar and they demonstrate similar mechanisms of activation and catalysis. Other allosteric pyruvate kinases that have been studied also behave as K-type systems with their effectors: *Trichomonas vaginalis* (Mertens et al., 1992); flounder liver (Sand, 1988); *Streptococcus lactis* (Crow & Pritchard, 1976); *Escherichia coli* Type 1 and 2 (Waygood & Sanwal, 1974; Waygood et al., 1975); *Mucor rouxii* (Passeron & Terenzi, 1970), and rat liver (Rozengurt et al., 1969). K-type pyruvate kinase systems appear to be ubiquitous in nature.

The heterotropic coupling parameters for the interactions of PEP, FDP, and Mn^{2+} with YPK were quantified using a kinetic linked-function analysis approach (Reinhart, 1983). A comparison of the coupling free energies and the dissociation constants obtained from this kinetic linked-function analysis with those obtained from a thermodynamic linked-function analysis (Mesecar & Nowak, 1997a) is shown in Table 5. The trend in the values for the coupling free energies is the same in both sets of studies. The interaction between PEP and FDP is weak ($\Delta G_{AX} = 0$ kcal/mol) in the absence of Mn^{2+}. In the absence of PEP, there is a positive interaction between the FDP and Mn^{2+} sites ($\Delta G_{XY} = -1.55$ kcal/mol) and in the absence of FDP, there is a larger, positive interaction between the PEP and Mn^{2+} sites ($\Delta G_{AY} = -2.75$ kcal/mol). Upon simultaneous binding of all three ligands, a substantial increase to -4.32 kcal/mol (ΔG_{AXY}) is observed.

One of the most notable coupling free energy values resulting from these analyses is the value of approximately 0 kcal/mol for the interaction between PEP and FDP with YPK. This value indicates that in the absence of Mn^{2+}, PEP, and FDP bind to the enzyme simultaneously and independently with little to no interaction between their binding sites. This result indicates that the free divalent metal plays a major role in modulating the allosteric responses of the enzyme. This is further exemplified by considering the coupling free energies between Mn^{2+} and PEP (-2.75 kcal/mol) and Mn^{2+} and FDP (-1.55 kcal/mol). The strong cooperative interactions between both of these ligand pairs results from the interaction of Mn^{2+} with YPK. In the presence of saturating Mn^{2+}, the coupling free energy between PEP and FDP ($\Delta G_{AX/Y}$) can be calculated from the following relationship: $\Delta G_{AX/Y} = \Delta G_{AXY} - \Delta G_{XY} - \Delta G_{AY}$. The resulting value of $\Delta G_{AX/Y}$ ($+0.30 \pm 0.39$ kcal/mol) indicates that, within experimental error, little or no interaction between the FDP and PEP sites exists even in the presence of saturating Mn^{2+}. The two ligand coupling free energies reveal that the binding of Mn^{2+} to the enzyme influences the binding of both FDP and PEP and that it does not influence to any appreciable extent the coupling between the FDP and PEP binding sites.

Differences in values between the two data sets may be due to larger experimental error associated with the kinetic studies or error in the various assumptions needed to treat the kinetic parameters as thermodynamic parameters. For instance, the Michaelis constant for PEP is highly dependent on the concentrations of both Mn^{2+} and FDP (Figures 2 and 7). The Michaelis constant for PEP decreases when the concentrations of Mn^{2+} and/or FDP are increased. At lower concentrations of Mn^{2+} and in the absence of FDP, the K_M for PEP increases to values above its dissociation constant. This implies that PEP may not be interacting with YPK in a rapid-equilibrium fashion but may be achieving binding equilibrium in the steady state. Ford and Robinson (1976) found, via tritium exchange studies with Mn^{2+} and FDP activated YPK at pH 6.2, that in the forward reaction approximately 9% of the tritium from tritiated PEP was found in water rather than in pyruvate. Approximately the same ratio of tritium in water to tritium in pyruvate was found for the rabbit muscle enzyme (Robinson & Rose, 1972). The results of these and other studies (Dann and Britton, 1978; Dougherty & Cleland, 1985) suggest that PEP is a "sticky" substrate for rabbit muscle PK and for YPK. As a result, the rate constant for dissociation of PEP would be slower than its turnover, making the Michaelis constant for PEP different than its dissociation constant.

An alternate explanation for the difference in the Michaelis constant and dissociation constant for PEP is that ADP antagonizes the binding of PEP. The presence of a saturating level of free ADP increases the dissociation constant for PEP 5-fold (Figure 6). The underlying mechanism for this antagonism may be the result of competition between PEP and ADP for the active site, ADP acting as a dead-end inhibitor, or the result of ADP binding to a distant allosteric site and negatively influencing the binding of PEP at the active site. The former would result in an infinitely positive coupling free energy if the binding of ADP and PEP is mutually exclusive. This appears not to be the case since the dissociation constant for PEP changes only by a factor of 5 in the presence of ADP yielding a coupling free energy between ADP and PEP of $+0.9 \pm 0.06$ kcal/mol. This finite and positive coupling free energy may result from the partial nature of allosteric inhibition (Reinhart, 1983) and is consistent with the latter argument. The presence of an ancillary nucleotide diphosphate binding site has been proposed by Waygood et al. (1976) for the allosteric *E. coli* enzyme from the results of equilibrium dialysis experiments, by Stuart et al. (1979) for the nonallosteric cat muscle enzyme on the basis of the crystal structure, by both Mildvan and Cohn (1966) and Rosevear et al. (1987) for the rabbit muscle enzyme using NMR techniques and by Cottam et al. (1972) for the yeast enzyme from results of both kinetic and direct binding studies. The possibility that free ADP complexes with YPK under catalytic conditions and influences the K_M for PEP is most probable. Clearly, the heterotropic influence of ADP on the allosteric kinetic parameters will have to be taken into account for a more complete kinetic description of the system.

The homotropic and heterotropic interactions described above cannot be explained by the simple two-state concerted model proposed by Monod et al. (1965). This model has failed to provide an adequate description for the ligand interactions of pyruvate kinase isolated from *E. coli* (Waygood et al., 1976) and *Saccharomyces carlsbergenesis* (Johannes & Hess, 1973). An extension of the sequential model proposed by Koshland et al. (1966) is necessary to

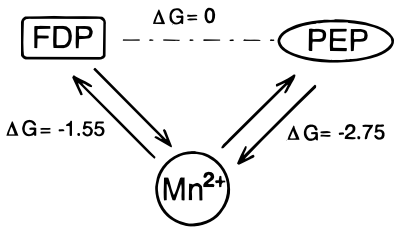

FIGURE 10: Allosteric relay mechanism for yeast pyruvate kinase illustrating the mechanism by which FDP influences the binding of PEP and vice versa. FDP and PEP positively influence the binding of each other on the enzyme surface by relaying the information through the enzyme bound metal. Direct interaction between the PEP and FDP sites is virtually nonexistent. The coupling free energies are given in kilocalories per mole.

fully describe this experimental data. In the third paper of this series (Mesecar & Nowak, 1997b), we illustrate how the Koshland model may be extended in order to accommodate the large number of conformational states that occur along a sequential pathway for YPK. However, analyzing the data in terms of free energy descriptions, the a priori assumption that the enzyme exists in two or more fixed conformational states was negated, and the magnitude of the multiple ligand interactions that exist with YPK were quantified.

Summary. The purported influence of FDP on the interaction of PEP may be explained by considering the model depicted in Figure 10. This model is based on the coupling free energies calculated in Table 4 and shows that the interaction of FDP with free YPK positively influences the binding of free Mn^{2+} and that the binding of Mn^{2+} positively influences the binding of PEP. The corollary is that PEP positively influences the binding of Mn^{2+} and then Mn^{2+} positively influences the binding of FDP. The binding of either PEP or FDP in the absence or presence of Mn^{2+} has little to no direct influence on the binding of the other ligand to its binding site. Thus, communication between the FDP and PEP sites occurs structurally through the metal site by means of an allosteric relay mechanism. The aforementioned results engender a new understanding into the nature of ligand interactions with YPK. The free divalent metal is largely responsible for coordinating the allosteric responses of the enzyme. This discovery may have important implications in understanding the role of metal cations in regulation of the glycolytic pathway where changes in the free divalent metal ion concentrations may directly result from changes in the ATP energy charge of the cell.

REFERENCES

Allen, S. C., & Muirhead, H. (1996) *Acta Crystallogr. D52*, 499−504.

Badwey, J. A., & Westhead, E. W. (1976) *J. Biol. Chem. 251*, 5600−5606.

Baek, Y. H., & Nowak, T. (1982) *Arch. Biochem. Biophys. 217*, 491−497.

Burke, R. L., Tekamp-Olson, P., & Najarian, R. (1983) *J. Biol. Chem. 258*, 2193−2201.

Caravjal, N., Gonzalez, R., Moran, A., & Oyarce, A. M. (1985) *Comp. Biochem. Physiolol. 82B*, 63−65.

Cottam, G. L., Mildvan, A. S., Hunsley, J. R., & Suelter, C. H. (1972) *J. Biol. Chem. 247*, 3802−3809.

Crow, V. L., & Pritchard, G. G. (1976) *Biochim. Biophys. Acta 438*, 90−101.

Dann, L. G., & Britton, H. G. (1978) *Biochem. J. 169*, 39−54.

Dougherty T. M., & Cleland, W. W. (1985) *Biochemistry 24*, 5875−5880.

Farber, G. K., & Petsko, G. A. (1990) *Trends Biochem. Sci. 15*, 228−234.

Ford, S. R., & Robinson, J. L. (1976) *Biochim. Biophys. Acta 438*, 119−130.

Fothergill-Gillmore, L. A. (1986) *Trends Biochem. Sci. 11*, 47−51.

Gonzalez, R., Carvajal, N., & Moran, A. (1984) *Comp. Biochem. Physiol. 78B*, 389−392.

Hunsley, J. R., & Suelter, C. H. (1969) *J. Biol. Chem. 244*, 4819−4822.

Johannes, K.-J., & Hess, B. (1973) *J. Mol. Biol. 76*, 181−205.

Johnson, J. J., & Reinhart, G. D. (1992) *Biochemistry 31*, 11510−11518.

Kinderlerer, J., Ainsworth, S., Morris C. N., & Rhodes, N. (1986) *Biochem. J. 234*, 699−703.

Klein, D. P., & Charles, A. M. (1989) *Curr. Microbiol. 19*, 57−60.

Koshland, D. E., Nemethy, G., & Filmer, D. (1966) *Biochemistry 5*, 365−385.

Kuczenski, R. T., & Suelter, C. H. (1971b) *Biochemistry 10*, 2862−2866.

Larsen, T. M., Laughlin, T., Holden, H. M., Rayment, I., & Reed, G. H. (1994) *Biochemistry 33*, 6301−6309.

Mattevi, A., Valentini, G., Rizzi, M., Speranza, M. L., Bolognesi, M., & Coda, A. (1996) *Structure 3*, 729−741.

Mertens, E., VanSchaftingen, E., & Muller, M. (1992) *Mol. Biochem. Parasitol. 54*, 13−20.

Mesecar, A. D., & Nowak, T. (1997a) *Biochemistry 36*, 6803−6813.

Mesecar, A. D., & Nowak, T. (1997b) *Biochemistry* (submitted for publication).

Mildvan, A. S., & Cohn, M. (1965) *J. Biol. Chem. 241*, 1178−1193.

Monod, J., Wyman, J., & Changeux, J. (1965) *J. Mol. Biol. 12*, 88−118.

Morris, C. N., Ainsworth, S., & Kinderlerer, J. (1986) *Biochem. J. 234*, 691−698.

Nowak, T., & Suelter, C. (1981) *Mol. Cell. Biochem. 35*, 65−75.

Passeron, S., & Terenzi, H. (1970) *FEBS Lett. 6*, 213−216.

Perrella, F. W. (1988) *Anal. Biochem. 174*, 437−447.

Reinhart, G. D. (1983) *Arch. Biochem. Biophys. 224*, 389−401.

Reinhart, G. D. (1985) *Biochemistry 24*, 7166−7172.

Reinhart, G. D. (1988) *Biophys. Chem. 30*, 159−172.

Rhodes, M., Morris, C. N., Ainsworth, S., & Kinderlerer, J. (1986) *Biochem. J. 234*, 705−715

Robinson, J. L., & Rose, I. A. (1972) *J. Biol. Chem. 247*, 1096−1105.

Rosevear, P. R., Fox, T. L., & Mildvan, A. S. (1987) *Biochemistry 26*, 3487−3493.

Rozengurt, E., Jimenez, L., de Asua, L. J., & Carminatti, H. (1969) *J. Biol. Chem. 244*, 3142−3147.

Sand, O. (1988) *Comp. Biochem. Physiol. 90*, 401−407.

Stuart, D. I., Levine, M., Muirhead, H., & Stammers, D. K. (1979) *J. Mol. Biol. 134*, 109−142.

Symcox, M. M., & Reinhart, G. D. (1992) *Anal. Biochem. 206*, 394−399.

Waygood, E. B., & Sanwal, B. D. (1974) *J. Biol. Chem. 249*, 265−274.

Waygood, E. B., Rayman, M. K., & Sanwal, B. D. (1975) *Can. J. Biochem. 53*, 444−454.

Waygood, E. B., Mort, J. S., & Sanwal, B. D. (1976) *Biochemistry 15*, 277−282.

Weber, G. (1972) *Biochemistry 11*, 864−878.

Weber, G. (1975) *Adv. Protein Chem. 29*, 1−83.

Yun, S.-L., & Suelter, C. H., (1976) *J. Biol. Chem. 251*, 124−128.

Zwaan, A. de, Holwerda, D. A., & Addink, A. D. F. (1975) *Comp. Biochem. Physiol. 52B*, 469−472.

BI962869T